Thermochimica Acta 613 (2015) 71–76

Contents lists available at ScienceDirect

Thermochimica Acta

journal homepage: www.elsevier.com/locate/tca

The assembly of dialkyldimethylammonium bromide cationic lipids as vesicles or monolayers in presence of poly(ethylene glycol)

Renata D. Adati, Eloi Feitosa*

Department of Physics, Sao Paulo State University, Sao Jose do Rio Preto, SP, Brazil

ARTICLE INFO

Article history:
Received 20 January 2015
Received in revised form 26 May 2015
Accepted 28 May 2015
Available online 1 June 2015

Keywords:
Differential scanning calorimetry
Dialkyldimethylammonium bromide salts
Poly(ethylene glycol)
Langmuir films
Polymer–surfactant interaction

ABSTRACT

The interaction between polymer and lipid vesicles may result in stabilization and formation of highly ordered networks, which can mimic biological membranes and be used as drug delivery system. Here we used differential scanning calorimetry (DSC) and Langmuir–Blodgett (LB) techniques to describe the effect of the nonionic water-soluble poly(ethylene glycol), PEG 35 kDa, on vesicles or monolayers from the cationic dialkyldimethylammonium bromide, D_nDAB (n = 12–18). Based on DSC data, up to 10 wt%, PEG plays minor role on the thermal behavior of D_nDAB, thus preserving the bilayer structure. Above 10 wt% PEG, there is no bilayer for n = 12–16, while for n = 18 there remains bilayer structures even in presence of 30 wt% PEG. The effect of PEG on the Langmuir monolayer of $D_{18}DAB$ depends on the amount of PEG in the sub-phase. In presence of up to ca 1 wt%, PEG yields more compressible films, while at higher polymer concentration the film is more extended and the collapse pressure is lower, most probably due to lipid solubility by the polymer solution. The PEG–D_nDAB complexes have potential application in controlled drug release by microgel nanoparticles.

1. Introduction

The self-assembly of synthetic cationic lipids from quaternary ammonium salts, such as dialkyldimethylammonium bromide (D_nDAB, n = 12, 14, 16, 18), into bilayer (*e.g.*, vesicles) or monolayer structures, are promising colloidal systems for industrial applications, with the advantage that they are low cost compounds [1,2]. One striking characteristics of these lipids is their melting temperature (T_m), which delineates the gel-to-liquid crystalline (LC) transition, which increases with the lipid chain length [1]. The reverse transition usually occurs at a lower temperature (T'_m), thus characterizing a thermal hysteresis the extent of which being characteristic of the lipids. The thermal behavior of D_nDAB bilayers [1], together with their monolayer characteristics [3], can be used to monitor the PEG–lipid interaction either in solution or at surface.

Cationic lipid vesicles are promising systems for drug delivery studies, especially after the pioneer work of Felgner et al. on the application of cationic lipid vesicles in nucleic acid delivery [4]. The interaction of cationic lipids with the anionic DNA or siRNA for lipoplex formation and transfection has been investigated [5,6].

In spite of optimizing the DNA cell transfection, polymer–lipid conjugates are widely used in the field of drug delivery to provide a polymer coat to confer favorable characteristics to the cell transfection. Poly(ethylene glycol), PEG, is a neutral polymer soluble in water as well as in some non-polar solvents, such as tetrahydrofuran, chloroform, dimethylsulfoxide or methanol [7]. The solubility in water makes PEG highly suitable for use in countless different applications in chemical, cosmetic and pharmaceutical industries [8].

Besides, PEG has been shown to stabilize the lamellar phase of lipoplexes, determining the efficiency in cell transfection [9,10]. Reports are available concerning preparation methods and physical stability of organized systems from didodecyldimethylammonium bromide ($D_{12}DAB$) and dioctadecyldimethylammonium bromide ($D_{18}DAB$) [11–13], while the characterization of bilayer structures from ditetradecyldimethylammonium bromide ($D_{14}DAB$) and dihexadecyldimethylammonium bromide ($D_{16}DAB$) has received minor attention [1,2].

Herein we focus on the interaction between neutral polymer and vesicle forming cationic lipids and describe the structural, thermal and kinetic behaviors of D_nDAB vesicles (n = 12–18) in the presence of PEG 35 kDa. The weak interaction between these compounds allows formation of vesicles in gel solution of PEG with potential use in controlled drug delivery.

* Corresponding author at: Department of Physics, São Paulo State University, Rua Cristovao Colombo, 2265, 15.054-000 Sao Jose do Rio Preto, SP, Brazil. Tel.: +55 17 3221 2238.
E-mail address: eloi@ibilce.unesp.br (E. Feitosa).

http://dx.doi.org/10.1016/j.tca.2015.05.022
0040-6031/

2. Experimental

2.1. Materials and methods

High purity >98% D_nDAB lipids were used: $D_{12}DAB$ (462.65 g mol^{-1}), $D_{14}DAB$ (518.74 g mol^{-1}), $D_{16}DAB$ (574.87 g mol^{-1}), and $D_{18}DAB$ (630.95 g mol^{-1}) were supplied by Sigma–Aldrich (St. Louis, USA) and used without further purification. Poly(ethylene glycol) 35 kDa (PEG) was purchased from Fluka (Buchs, Switzerland). Ultra-pure Milli-Q® water quality (resistivity 18.2 MΩ cm) was used in sample preparation and in the Langmuir film experiments.

2.2. Vesicle preparation

Dispersions were obtained from D_nDAB at 5.0 mM prepared in water in the absence or in presence of up to 30 wt% PEG. Mixtures of D_nDAB/water or D_nDAB/PEG solution were gently stirred magnetically for 1 h at a temperature safely above the melting temperature (T_m) from the lipids [1]. Accordingly, $D_{12}DAB$ dispersions were prepared at 25 °C, $D_{14}DAB$ and $D_{16}DAB$ at 35 °C, and $D_{18}DAB$ at 60 °C.

2.3. DSC measurements

A VP-DSC Microcalorimeter (Microcal Inc., Northampton, MA, USA) was used to collect data and the Origin® 7.0 software (supplied by the manufacturer) was used to record and to analyze the data. The experiments were performed by heating and cooling the sample and reference at the desired scan rate (60 or 20 °C/h, respectively for the shorter or the longest lipid chain length) in the temperature range of 1–65 °C. The thermograms were recorded as change in heat capacity at constant pressure, as a function of temperature. The transition enthalpies, ΔH(kJ mol^{-1}), were calculated from the area under the peaks, and the temperature at the peak maximum was taken as the transition temperature. The shape of the curve gives additional information about the phase transition and the width at half-height ($\Delta T_{1/2}$) is related to the cooperatively of the transition, which is higher the narrower is the peak. The DSC scans were obtained in duplicate to check reproducibility. More details about the experimental setup can be found elsewhere [11].

2.4. Langmuir films

The surface pressure–area (π–A) isotherms of the Langmuir films were obtained using a KSV-NIMA Langmuir balance. The monolayers were formed by spreading 50 μL of a 0.30 mg mL^{-1} $D_{18}DAB$ chloroform solution on the air/water or air/aqueous solution of up to 10 wt% PEG in the sub-phase. The solvent was allowed to evaporate for 10 min prior to sweeping the surface with the movable barriers. The π–A isotherms were recorded using a barrier speed of 10 mm min^{-1}. All experiments were carried out at room temperature (25 ± 1 °C).

3. Results and discussion

3.1. $D_{12}DAB$/PEG

Fig. 1 shows DSC thermograms for 5 mM (0.23 wt%) $D_{12}DAB$ dispersions in the absence and presence of up to 30 wt% PEG obtained in the heating mode using a 12 h pre-scan time. This rather long pre-scan time was used because of the slow (LC-to-gel) cooling transition [14–16]. The gel-to-LC transition temperature of $D_{12}DAB$ is well defined giving a very sharp single endotherm around $T_m \approx 16.0$ °C, with peak width $\Delta T_{1/2} < 1$ °C, in the DSC trace,

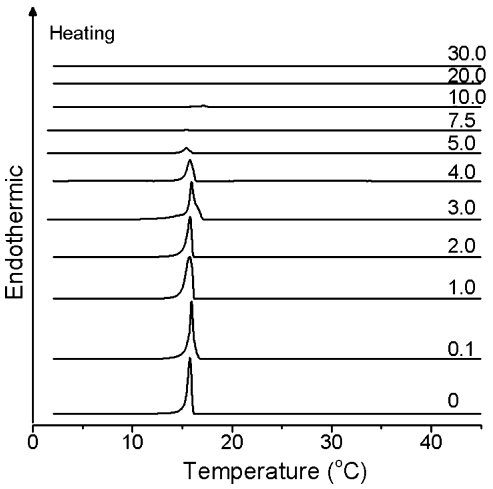

Fig. 1. Heating DSC thermograms for $D_{12}DAB$ aqueous dispersions at 5.0 mM in the absence and presence of up to 30 wt% PEG. Input DSC parameters: pre-scan time 12 h and scan rate 20 °C/h.

indicating high cooperativity of this transition. The reverse LC-to-gel transition, however, has not been detected directly by DSC (or any other technique) because of its very slow kinetics even though it has been detected indirectly as a broad exotherm around $T_m \approx 9.5$ °C [16]. In water $D_{12}DAB$ thus displays a thermal hysteresis of 6.5 °C.

By adding PEG, T_m tends to decrease indicating $D_{12}DAB$-PEG interaction, leaving the $D_{12}DAB$ bilayer more fluid. In presence of up to 4 wt% PEG, the T_m value does not change appreciably ($T_m \approx 16$ °C), but it decreases slightly to a minimum of 13.3 °C when PEG concentration attains 5.0 wt% (Fig. 2).

The enthalpy change (ΔH_m) related to the gel-to-LC transition decreases steeply from 54 to 1.5 kJ mol^{-1} when PEG concentration was raised from 4.5 to 7.5 wt% (Fig. 2). Above this concentration there is no vesicle. We ascribe the decrease in enthalpy to the reduction of the relative amount of vesicles. The lipids sequestered from the vesicles are probably complexing with PEG molecules despite the reported weak affinity of PEG to micelle-forming cationic surfactants [17]. The structure determination of these complexes is beyond the scope of the present work which focus on the vesicle structure in presence of PEG.

3.2. $D_{14}DAB$/PEG

Vesicles from $D_{14}DAB$ (together with $D_{16}DAB$) are the less investigated from the D_nDAB series most probably because of their low stability in water. The reason these vesicles are more unstable

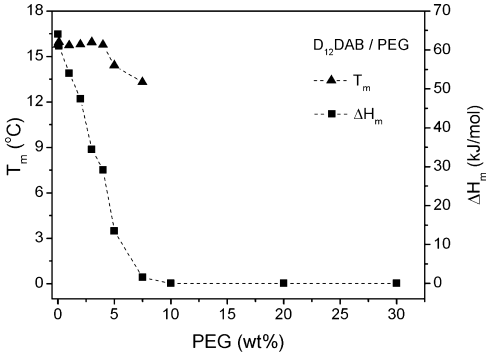

Fig. 2. Effect of PEG concentration on the melting temperature (T_m) and the enthalpy (ΔH_m) of $D_{12}DAB$ at 5 mM.

is still a matter of investigation. Similar to D_{12}DAB, D_{14}DAB also displays slow LC-to-gel transition [15] and its reverse LC-to-gel transition temperature has not been reported so far by DSC or other technique.

Fresh D_{14}DAB dispersions both in water and in PEG solution are homogeneous and optically clear, whereas dispersions equilibrated for about one week after preparation present some crystal precipitates. This indicates that PEG plays minor role on the stabilization of these vesicles. Because of such instability we worked here with fresh dispersions of D_{14}DAB. All samples were homogenized by manually shaking the recipients at room temperature prior pouring them into the DSC cell.

Fig. 3 shows heating DSC thermograms for 5 mM D_{14}DAB in water and in presence of up to 30 wt% PEG, obtained in the temperature range 1–55 °C, pre-scan time 15 min, and scan rate 60 °C/h. Under similar condition, in the cooling mode, it was detected no reverse transition (thermograms not shown), probably due to the slow kinetics of this transition [15]. On heating, D_{14}DAB vesicles in water display two main transitions at T_s = 13.7 °C and at T_m = 29.4 °C. Similar to D_{18}DAB [11] and according to Ref. [15], most probably these transitions are related to the gel-to-tilt (intermediate) transition and tilt-to-LC transition, respectively. Similar to D_{12}DAB, in the presence of up to 0.1 wt% PEG, T_m does not vary considerably, while the transition enthalpy decreases steeply (Table 1).

Between 10 and 20 wt% PEG the thermograms display no endotherm, indicating that there is no vesicle in the solution. The decrease in enthalpy (ΔH_s or ΔH_m) indicates that the amount of vesicles decreases as PEG concentration increases. The slight decrease in T_m to ca 28.0 °C suggests weak interaction, which may occur on the vesicle surface without penetration of the polymer into the bilayer (Table 1).

3.3. D_{16}DAB/PEG

Like D_{14}DAB vesicles, D_{16}DAB vesicles are quite unstable. According to Fig. 4a, both in the absence and presence of PEG, the heating thermograms display up to two main transitions at T_m = 28.5 °C and T_p = 42.1 °C. In parallel with D_{18}DAB, we associated these transitions to the gel-to-LC transition for the vesicle and multi-lamellar structures, respectively [11]. In the presence of up to 10 wt%, PEG affects only slightly the T_m and T_p values. Between 10 and 20 wt% PEG, there is no remaining vesicle (no thermal transition). All thermal peaks are rather sharp ($\Delta T_{1/2}$ < 1.1 °C) and

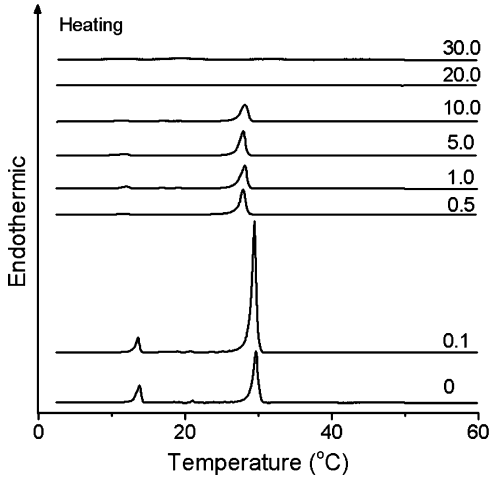

Fig. 3. Heating DSC thermograms for D_{14}DAB aqueous dispersions at 5.0 mM in the absence and presence of up to 30 wt% PEG. Input DSC parameters: pre-scan time 15 min and scan rate 60 °C/h.

Table 1
Thermal parameters of D_{14}DAB (5.0 mM)/PEG, obtained from analyses of the heating DSC thermograms in Fig. 3.

PEG (wt%)	T_s (°C)	ΔH_s (kJ mol^{-1})	$\Delta T_{s,1/2}$ (°C)	T_m (°C)	ΔH_m (kJ mol^{-1})	$\Delta T_{m,1/2}$ (°C)
0	13.5	2.11	0.5	29.4	23.4	0.7
0.1	13.7	2.09	0.7	29.6	9.9	0.7
0.5	–	–	–	27.9	5.5	0.8
1.0	–	–	–	28.1	5.4	1.0
5.0	–	–	–	27.9	5.2	0.8
10	–	–	–	28.2	4.2	1.1

there we found no clear dependence of the peak width ($\Delta T_{1/2}$) on PEG concentration. Further, similar to D_{14}DAB, PEG does not affect the vesicle stability. The thermal parameters obtained from the analyses of the heating and cooling traces are summarized in Tables 2 and 3, respectively.

On cooling, the thermograms display two exotherms (Fig. 4b), a narrow one at T'_m = 22.9 °C ($\Delta T_{1/2}$ < 0.6 °C) and a broader one around $T'_p \approx 15$ °C ($\Delta T_{1/2}$ > 2.0 °C). We hypothesize that the T'_m-transition is the reverse to the T_m-transition (hysteresis ΔT_m = 5.7 °C), while the T'_p-transition is the reverse to the T_p-transition (hysteresis $\Delta T_p \approx 27$ °C). These findings are in line with those reported previously for D_{18}DAB [18]. As expected, PEG does not affect considerably these hysteresis values (Tables 2 and 3).

Concerning the transition enthalpies we notice that surprisingly the T_m-transition is about two-fold more energetic than its reverse T'_m-transition, while it is much lower for the T_p-transition than for its reverse T'_p-transition (Tables 2 and 3). Despite that, the total heating and cooling enthalpies are about the same, 70–75 kJ mol^{-1}. The reason for this behavior is not clear, but may be related to the appearance of additional transitions at temperatures above T_p (which appear like noise in Fig. 4a), which may be related to the vesicle instability.

3.4. D_{18}DAB/PEG

We finally investigated the interaction of PEG with the longest lipid D_{18}DAB, which is the most investigated lipid of the series D_nDAB. Fig. 5a and b shows respectively some heating and cooling DSC thermograms for D_{18}DAB at 5 mM in water and in presence of up to 30 wt% PEG. On heating (Fig. 5a), the thermogram of PEG-free D_{18}DAB presents a gel-to-tilt and a tilt-to-LC transitions, ascribed to the lipid chain tilting and melting, at $T_s \approx 36$ °C and $T_m \approx 45$ °C, respectively [11,18].

In presence of PEG, T_s decreases by up to 2.5 °C, while T_m increases by up to 1 °C. A third endotherm at T_p = 52 °C due to the gel–LC transition of the lamellar (Lam) structures can be seen for D_{18}DAB 5 mM both in the absence and presence of PEG. As the enthalpy ΔH_p tends to increase with increasing PEG concentration, we can say that PEG favors the lamellar rather than the vesicle (Ves) structure. $T_p > T_m$ implies that the Lam bilayers are less fluid than the Ves bilayers. On cooling, reverse transitions at T'_m and T'_s, were detected at around 40 and 9–11 °C, respectively. The T'_p-exotherm is positioned at $T'_p = T'_m$, as reported [18].

The heating thermograms for D_{18}DAB at 5 mM in presence of up to 30 wt% PEG show additional secondary transitions (like noise signals) mainly above T_m. This indicates that even at such a high viscous solution there still remains vesicles mixed with more complex structures (most probably multi-lamellae) because of the existing T_p-transition. The thermal parameters obtained from the analyses of these traces are summarized in Tables 4 and 5, respectively for the heating and cooling processes.

The similarity of the heating thermograms for D_{18}DAB at 5 mM in water and in presence of PEG (displaying three main endotherms), together with the single exotherm around 40 °C in

Table 2
Thermal parameters of $D_{16}DAB$ (5.0 mM)/PEG dispersions obtained from the analyses of the heating thermograms in Fig. 4a.

PEG (wt%)	T_m (°C)	ΔH_m (kJ mol^{-1})	$\Delta T_{m,1/2}$ (°C)	T_p (°C)	ΔH_p (kJ mol^{-1})	$\Delta T_{p,1/2}$ (°C)
0	28.6	71.3	0.6	42.1	3.9	1.1
0.1	28.5	70.0	0.7	42.1	5.1	1.0
1.0	28.5	63.2	0.5	42.2	8.0	0.9
5.0	28.3	59.0	0.7	42.1	16.3	0.9
10	28.1	56.1	0.8	42.0	9.4	1.3

Table 3
Thermal parameters of $D_{16}DAB$ (5.0 mM)/PEG dispersions obtained from the analyses of the cooling thermograms in Fig. 4b.

PEG (wt%)	T'_p (°C)	$\Delta H'_p$ (kJ mol^{-1})	$\Delta T'_{p,1/2}$ (°C)	T'_m (°C)	$\Delta H'_m$ (kJ mol^{-1})	$\Delta T'_{m,1/2}$ (°C)
0	14.9	36.8	2.2	22.9	34.8	0.5
0.1	14.9	36.8	2.5	23.0	34.8	0.5
1.0	14.6	33.7	2.7	23.0	32.5	0.5
5.0	14.5	36.3	4.9	23.0	34.5	0.6
10	15.7	32.3	4.1	23.0	32.4	0.6

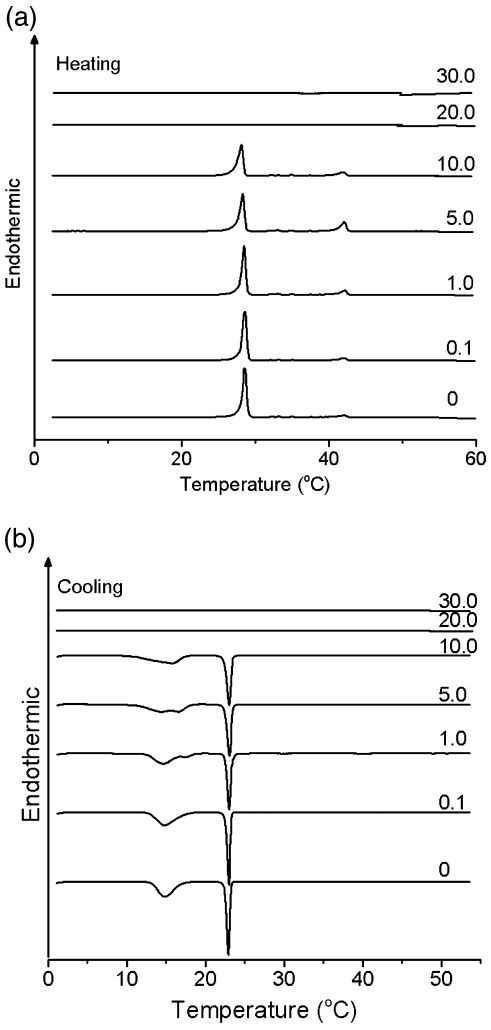

Fig. 4. Effect of PEG on the heating (a) and cooling (b) DSC thermograms for $D_{16}DAB$ at 5.0 mM. Input data: pre-scan time 15 min; scan rate 60 °C/h.

the cooling thermograms, point to the formation of vesicles and lamellae in the viscous media of PEG, with similar structure to those formed in water [11]. Such vesicles in PEG gel solution may find application in controlled drug delivery [19].

Table 6 summarizes the figures on the effect of PEG on the D_nDAB vesicle properties, lipid complete solubilization and vesicle stability induced by PEG. The most outstanding characteristic is that the amount of PEG necessary to solubilize completely the bilayer lipids increases with the lipid chain length. Therefore, $D_{18}DAB$ vesicles are the most resistant to PEG. Furthermore, at concentrations below that of complete lipid solubilization, PEG plays minor role on the vesicle stability. Interestingly, these vesicles can be formed in gel solution of PEG at concentration as high as 30 wt%, while the shorter $D_{12}DAB$ requires only about 7.5 wt % PEG to be solubilized completely.

3.5. Langmuir films

D_nDAB lipids with shorter chains ($n < 18$) are soluble in water and therefore poorly air/water surface-active. Therefore, they are not suitable to assemble as monolayer. The longest $D_{18}DAB$ has lower solubility in water and is more appropriate to assemble as monolayer at the air/water surface. We then investigated $D_{18}DAB$ monolayers for the aqueous sub-phase containing or not up to 10 wt% PEG

The interfacial $D_{18}DAB$ organization was monitored by the π–A isotherm, as shown in Fig. 6 for selected PEG concentrations in the sub-phase. Accordingly, with PEG in the sub-phase, the liquid-expanded (LE) phase is more extended as evidenced by the shift of the isotherm to the left, and the collapse occurs at lower surface pressure (37 mN m^{-1}) relative to pure water (45 mN m^{-1}). Furthermore, differently from pure water, PEG leaves constant the surface pressure after the collapse, again evidencing the PEG–$D_{18}DAB$ interaction.

In the presence of up to 1.0 wt% PEG, the monolayer is more compressible and as a result the isotherm is shifted to lower area per molecule. This indicates some miscibility between the lipids from the monolayer with the polymers next to the surface. In the presence of 0.1 wt% PEG, the lipids are considerably more densely packed, probably because the polymers drain some water molecules from the monolayer interfaces, thus promoting compaction of the lipids. At higher PEG concentrations (2.0–5.0 wt%), the monolayer becomes slightly more expanded and the LE-to-LC transition is more evident. This result can be explained by the polymer network formation, leaving the monolayer less stable.

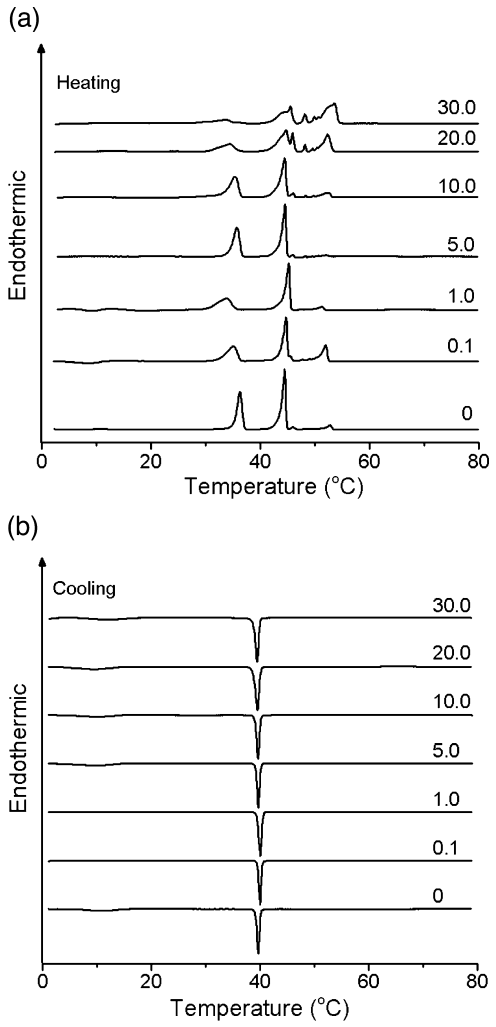

Fig. 5. Heating (a) and cooling (b) DSC thermograms for D_{18}DAB at 5.0 mM in presence of up to 30 wt% PEG. Inputs: pre-scan time 15 min; scan rate equals 60 °C/h.

Therefore, the D_{18}DAB assembly as expanded monolayer may be due to the increase in the lipid solubility.

At even higher PEG concentration (*e.g.*, 10 wt%), the isotherm profile changes considerably, becoming flattened and there appears no clear LC–LE transition, probably at this concentration, the film cannot be structured in a similar way to that in the absence of PEG, because of the higher lipid solubility in the PEG solution and the lipids is even less densely packed in the monolayer, resulting in much lower collapse pressure (Fig. 6). The change in miscibility of the lipids in PEG solution demonstrates high potential application of the lipid organization as monolayer or bilayer (vesicles) to the control of drug release, which can be tuned by adjustable amount of polymer (PEG) in solution.

4. Conclusions

Despite the expected weak interactions between the nonionic PEG 35 kDa and the cationic D_nDAB (n = 12–18), our DSC and Langmuir film data clearly point to the following main conclusions: D_nDAB vesicles are formed in PEG solution. The amount of vesicles decreases with increasing PEG concentration owing to lipid solubilization (sequestering) by the polymer solution. The PEG concentration necessary to completely solubilize the vesicles of D_nDAB increases with increasing the lipid chain length: around 7.5 mM for D_{12}DAB, 10–20 mM for D_{14}DAB and D_{16}DAB), and >30 mM for D_{18}DAB. This indicates higher stability of the longest D_{18}DAB vesicles in PEG solution, what may be related to stronger hydrophobic effects. D_{18}DAB monolayer is more extended in presence of up to 1 wt% PEG in the sub-phase, while above 5 wt% PEG the isotherm is flattened indicating lipid solubilization (sequestering) by the polymer solution. PEG also lowers the collapse surface pressure and raises the molecular area, also indicating polymer–lipid interactions.

The assembly of lipids into vesicles or monolayers in aqueous environments may find useful applications in nanomedicine as the assembled structures themselves display detached functions in drug delivery, and the aqueous moiety in which such structures are embedded, may function stabilizer for the colloidal complexes. Therefore, vesicle in polymer environments can be useful in preparation of nanostructures for controlled drug delivery [19].

Table 4
Thermal parameters of D_{18}DAB (5.0 mM)/PEG obtained from analyses of the heating thermograms in Fig. 5a.

PEG (wt%)	T_s (°C)	ΔH_s (kJ mol^{-1})	$\Delta T_{s,1/2}$ (°C)	T_m (°C)	ΔH_m (kJ mol^{-1})	$\Delta T_{m,1/2}$ (°C)	T_p (°C)	ΔH_p (kJ mol^{-1})	$\Delta T_{p,1/2}$ (°C)
0	36.3	35.1	1.1	44.1	38.9	0.8	52.9	3.8	0.9
0.1	35.8	31.2	1.7	44.5	39.7	0.8	52.3	14.5	1.1
1.0	35.9	26.8	1.1	44.4	31.5	0.8	51.9	4.4	1.9
5.0	35.7	35.4	1.4	44.5	40.8	0.8	52.1	3.3	3.2
10	35.4	32.3	1.8	44.4	41.5	1.1	52.5	7.0	1.9
20	34.4	18.0	3.1	44.7	41.9	1.9	52.3	22.4	1.3
30	33.6	13.9	4.4	45.5	30.0	2.4	53.5	47.4	2.4

Table 5
Thermal parameters of D_{18}DAB (5.0 mM)/PEG obtained from analyses of the cooling thermograms in Fig. 5b.

PEG (wt%)	T'_s (°C)	$\Delta H'_s$ (kJ mol^{-1})	$\Delta T'_{s,1/2}$ (°C)	ΔT_s (°C)	T'_m (°C)	$\Delta H'_m$ (kJ mol^{-1})	$\Delta T'_{m,1/2}$ (°C)	ΔT_m (°C)
0	11.3	14.3	5.0	25.1	39.7	40.7	0.5	4.4
0.1	9.4	2.8	5.4	26.2	40.1	43.5	0.5	4.7
1.0	11.5	15.3	4.4	24.4	39.7	36.2	0.5	4.7
5.0	9.9	18.8	6.3	25.8	39.8	42.8	0.5	4.7
10	10.3	17.4	6.0	25.1	39.6	43.8	0.6	4.8
20	9.3	21.8	7.0	25.1	39.5	48.7	0.8	5.2
30	12.4	14.6	5.7	21.2	39.5	47.0	0.7	6.0

Table 6
Summary of parameters related with the solubilization of D_nDAB lipids by PEG solution.

Alkyl chain length (n)	Stability	T_m (°C)	ΔH_m (kJ mol^{-1})	$T_{m,sol}$ (°C)	$\Delta H_{m,sol}$ (kJ mol^{-1})	PEG conc. (wt%)
12	Yes	15.9	65	13.3	1.5	7.5
14	<One week	29.4	23.4	28.2	4.2	10–20
16	<One week	28.6 (42.2)	71.3 (3.9)	28.1 (42.0)	56.1 (9.4)	10–20
18	Yes	44.1	38.9	45.5	30.0	>30

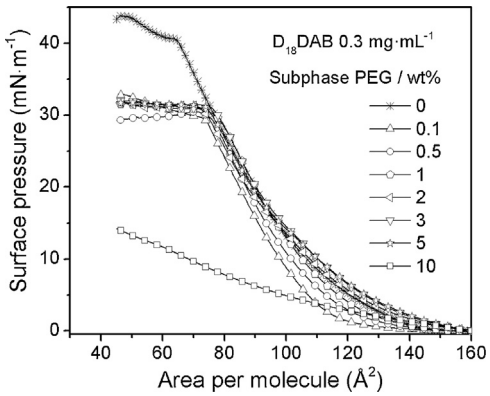

Fig. 6. π–A isotherms for injection of 50 μL 0.30 mg mL^{-1} D_{18}DAB chloroform solution on the PEG solution in the sub-phase. The PEG concentrations are indicated on the figure.

Acknowledgments

R.D.A thanks FAPESP for grant (2011/07414-0). E.F. thanks FAPESP (2011/03566-0) and CNPq (303030/2012-7).

References

[1] E. Feitosa, J. Jansson, B. Lindman, The effect of chain length on the melting temperature and size of dialkyldimethylammonium bromide vesicles, Chem. Phys. Lipids 142 (2006) 128–132.
[2] M.J. Blandamer, B. Briggs, P.M. Cullis, B.J. Rawlings, J.B.F.N. Engberts, Vesicle–cholesterol interactions: effects of added cholesterol on gel-to-liquid crystal transitions in a phospholipid membrane and five dialkyl-based vesicles as monitored using DSC, Phys. Chem. Chem. Phys. 5 (2003) 5309–5312.
[3] A. Cavelli, P. Dynarowicz-Łątka, O.N. Oliveira Jr, E. Feitosa, Using an effective surface charge to explain surface potentials of Langmuir monolayers from dialkyldimethylammonium halides with Gouy–Chapman theory, Chem. Phys. Lett. 338 (2006) 88–94.
[4] P.L. Felgner, T.R. Gadek, M. Holm, R. Roman, H.W. Chan, M. Wenz, J.P. Northrop, G.M. Ringold, Lipofection: a highly efficient, lipid-mediated DNA-transfection procedure, Proc. Natl. Acad. Sci. U. S. A. 84 (1987) 7413–7417.
[5] C.R. Dass, T.L. Walker, M.A. Burton, Liposomes containing cationic dimethyldioctadecyl ammonium bromide: formulation, quality control and lipofection efficiency, Drug Deliv. 9 (2002) 11–18.
[6] A.C.N. Oliveira, T. Martens, K. Raemdonck, R.D. Adati, E. Feitosa, C. Botelho, A.C. Gomes, K. Braeckmans, M.E.C.D. Real Oliveira, Dioctadecyldimethylammonium:monoolein nanocarriers for efficient in vitro gene silencing, ACS Appl. Mater. Interfaces 6 (2014) 6977–6989.
[7] C. Özdemir, A. Güner, Solubility profiles of poly(ethylene glycol)/solvent systems, I: qualitative comparison of solubility parameter approaches, Eur. Polym. J. 43 (2007) 3068–3093.
[8] J.M. Harris, Poly(ethylene glycol) Chemistry: Biotechnical and Biomedical Applications, Plenum Press, New York, 1992.
[9] Y. Xu, S.W. Hui, P. Frederik, F.C. Scoza Jr., Physicochemical characterization and purification of cationic lipoplex, Biophys. J. 77 (1999) 341–353.
[10] S.H. Jung, S.H. Jung, H. Seong, S.H. Cho, K.S. Jeong, B.C. Shin, Polyethylene glycol-complexed cationic liposome for enhanced cellular uptake and anticancer activity, Int. J. Pharm. 382 (2009) 254–261.
[11] E. Feitosa, R.D. Adati, P. Hansson, M. Malmsten, Thermal and structural behavior of dioctadecyldimethylammonium bromide dispersions studied by differential scanning calorimetry and X-ray scattering, Plos One 7 (9) (2012) e44702.
[12] E. Feitosa, F.R. Alves, A. Niemiec, M.E.C.D. Real Oliveira, E.M. Castanheira, A.L. Baptista, Cationic liposomes in mixed didodecyldimethylammonium bromide and dioctadecyldimethylammonium bromide aqueous dispersions studied by differential scanning calorimetry, nile red fluorescence, and turbidity, Langmuir 22 (2006) 3579–3585.
[13] G. Angelini, M. Chiarini, P. De Maria, A. Fontana, C. Gasbarri, G. Siani, D. Velutto, Characterization of cationic liposomes. Influence of the bilayer composition on the kinetics of the liposome breakdown, Chem. Phys. Lipids 164 (2011) 680–687.
[14] E. Feitosa, Kinetic asymmetry in the gel–liquid crystalline state transitions of DDAB vesicles studied by differential scanning calorimetry, J. Colloid Interface Sci. 344 (2010) 70–74.
[15] M.J. Blandamer, B. Briggs, P.M. Cullis, S.D. Kirby, J.B.F.N.J. Engberts, Reorganisation of alkyl chains in vesicles formed in aqueous solution by dialkyldimethylammonium bromide, R2N+Me2Br- where R=C12H25, C14H29, C16H33 or C18H37, Chem. Soc. Faraday Trans. 93 (1997) 453–455.
[16] E. Feitosa, R.D. Adati, F.R. Alves, Thermal and phase behavior of didodecyldimethylammonium bromide aqueous dispersions, Colloids Surf. A: Physicochem. Eng. Aspects (2015), doi:http://dx.doi.org/10.1016/j.colsurfa.2015.01.086. (in press) http://www.sciencedirect.com/science/article/pii/S0927775715001144.
[17] K. Hayakawa, J.C.T. Kwak, Interactions between polymers and cationic surfactants, in: D. Rubingh, P.M. Holland (Eds.), Cationic Surfactantas Physical Chemistry, Marcel Dekker, New York, 1991.
[18] E. Feitosa, R.D. Adati, Reversibility of thermal transitions in dilute dioctadecyl-dimethyl-ammonium bromide vesicles, J. Surfact. Deterg. 17 (2014) 1055–1058.
[19] V.B. Bueno, L.H. Catalani, K.R.P. Daghastanli, I.M. Cuccovia, H. Chaimovich, Preparation of PVP hydrogel nanoparticles using lecithin vesicles, Quim. Nova 33 (2010) 2083–2087.